Time-Invariant Strategies in Coordination of Human Reaching

Satyajit Ambike and James P. Schmiedeler

Department of Mechanical Engineering, The Ohio State University, Columbus, OH 43210, U.S.A., e-mail: {ambike.1, schmiedeler.2}@osu.edu

Abstract. This paper addresses validation of a curvature-theory-based time-invariant inverse kinematic model and a related tracking algorithm for human motor control of reaching motions. Human subjects made unconstrained reaching motions in the horizontal plane to fixed targets at three self-selected speeds. Consistent shoulder/elbow joint speed ratios for motions to the same target across speeds were observed, indicating a time-invariant planning strategy. The inverse kinematic model's technique of relating joint motions with a Taylor series expansion is in concert with the leading joint hypothesis. With this approach the tracking algorithm successfully replicated the experimental wrist trajectories, and also predicted the previously observed elbow-led motions for reaching in the ipsilateral hemifield. The elbow leads the arm motion in this hemifield because the shoulder approaches a dwell. A computationally frugal strategy of intermittent path correction based on two error parameters is proposed.

Key words: curvature theory, motor control, arm kinematics, leading joint hypothesis.

1 Introduction

It has been proposed that the fundamental internal model employed by the human central nervous system (CNS) for motor coordination of reaching motions is a time-invariant inverse kinematic model [1] that can be mathematically described using two-degree-of-freedom curvature theory for planar motions [8]. This mathematical model matches the instantaneous geometric properties of the desired wrist path to the instantaneous geometric properties of a corresponding path in the joint space of the mechanism, i.e. the human arm. The elbow and shoulder joint motions are coordinated through a Taylor series expansion such that one joint leads, and the other is subordinate. This approach is implemented to track paths of arbitrary length within a planar mechanism's workspace via a tracking algorithm [2]. The use of the Taylor series to relate joint motions echoes the recent leading joint hypothesis (LJH) [5] which states that in multi-joint limb motion one joint, usually the proximal joint, acts as a leading joint by moving independent of the other joints. The subordinate joints then move such that the required end-effector motion is achieved. This hypothesis grew in part from the work of Levin et al. [7] and Dounskaia et al. [4],

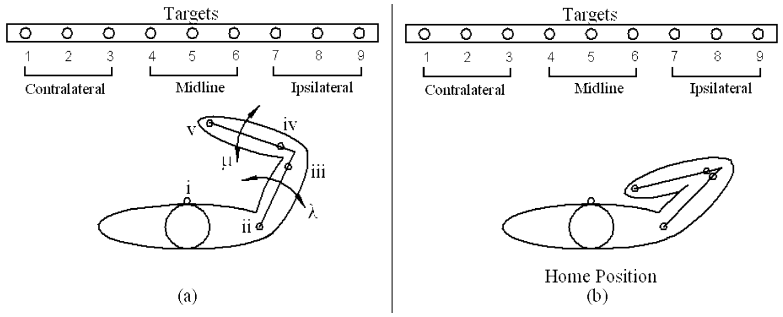

Fig. 1 Schematic of experiment; (a) sensor locations with roman numerals – λ and μ indicate upper and forearm angular displacements from their current positions; (b) the home position.

who also found that the shoulder is the leading joint for most hand movements in the horizontal plane. Movements in the the ipsilateral hemifield are elbow-led. This paper analyzes data from horizontal reaching motions performed by healthy human subjects to validate the time-invariant model and the path-tracking algorithm.

2 Experimental Methods

Thirteen subjects with no history of neurological injury participated in this study, complete details of which are in [3]. As shown in Figure 1, subjects sat upright facing a set of nine targets (incandescent lights) arranged equidistantly along a horizontal line. The targets were positioned with the fifth light in the subject's mid-line sagittal plane. An electromagnetic spatial tracking system recorded arm motions with sensors placed at the sternum, shoulder (scapula), lower bicep, upper forearm, and wrist (midpoint between the ulnar and radial styloids).

Each test began with the subject's arm in a horizontal home position as shown in Figure 1b, with the elbow bent to place the tip of the index finger near the sternum marker (marker *i* in Figure 1a). A single target was illuminated, followed by an audio cue of 'slow', 'normal', or 'fast', indicating the speed with which to reach toward the target. Normal indicated the subject's natural speed, while slow and fast indicated exaggerated deviations from normal. The subject extended the arm to point at the target and returned to the home position. Subjects were instructed to maintain the horizontal orientation of the arm during the motion and to consistently use the same three speeds throughout the experiment. The sequence of target illumination and the speed cues was predefined, but unknown and seemingly random to the subject. The subjects were unrestrained, but were instructed to keep their torsos as steady as possible, especially for contralateral reaching. The experiment ended when the subject had pointed to all nine lights at all three speeds, first with the right hand and then with the left, yielding 27 tests for each hand.

3 Model and Algorithm Validation

The following analysis aims to validate the hypothesis that the authors' two-degree-of-freedom (DOF) curvature-theory model [8], along with their tracking algorithm [2] can describe the internal inverse-kinematic model used by the CNS for planar arm motions. The algorithm enables planar path tracking with two-DOF planar mechanisms. Consequently, the human arm is modeled as a planar revolute-revolute (RR) mechanism, with the shoulder and elbow being parallel-axis revolutes. A planar trajectory best representing the 3-dimensional wrist (marker v in Figure 1a) data, called the *experimental path*, is first obtained. The validation is done by demonstrating that a fourth-order polynomial fit to the experimental path, called the *desired path*, can be tracked using the algorithm. The algorithm tracks the desired path using an equivalent RR mechanism, the parameters of which, viz. the arm segment lengths and the fixed shoulder location, are input to the algorithm. These are obtained by analyzing the marker data from each test. The arm lengths for a particular subject are constant, but the shoulder location varies for each test, as described below. The tracking results indicate that the algorithm can effectively track the desired paths. The experimental speed ratios, defined later, are obtained from the experimental path via inverse kinematics, and the algorithm generates the modeling speed ratios based on the desired path. Comparison of the experimental and modeling speed ratios provides corroboration for the LJH.

3.1 Data Analysis and Experimental Speed Ratios

This section describes the methodology to obtain planar experimental and desired paths, the equivalent RR mechanism for each test, and the joint trajectories and speed ratios for tracking the experimental paths.

To obtain the experimental and desired paths, the motion of all the arm markers is first expressed in a sternum-marker-fixed frame to eliminate any artifact due to small torso movements. Next, the portion of the data with no arm motion, which occurs at the beginning, at the end, and briefly at full arm extension, is eliminated. A best-fit plane, termed the *motion plane*, is obtained such that the distance between the position data of all the markers and the plane is minimized in a least-squares sense. Each test has a unique motion plane onto which the data is projected. The arm motion for each test is considered to lie entirely in its corresponding motion plane. The projected wrist (marker v in Figure 1a) data is the experimental path, and the fourth-order polynomial fit to the experimental path serves as the desired path.

The parameters of the equivalent mechanism are obtained as follows. To obtain the forearm length, the motion of the wrist (marker v in Figure1a) relative to the upper arm (marker iii in Figure1a) is plotted. This relative wrist path is assumed to be a circular arc of radius equal to the distance from the elbow to marker v, and a circle is fit in the least-squared sense [6] to each of the 27 relative wrist paths. The arith-

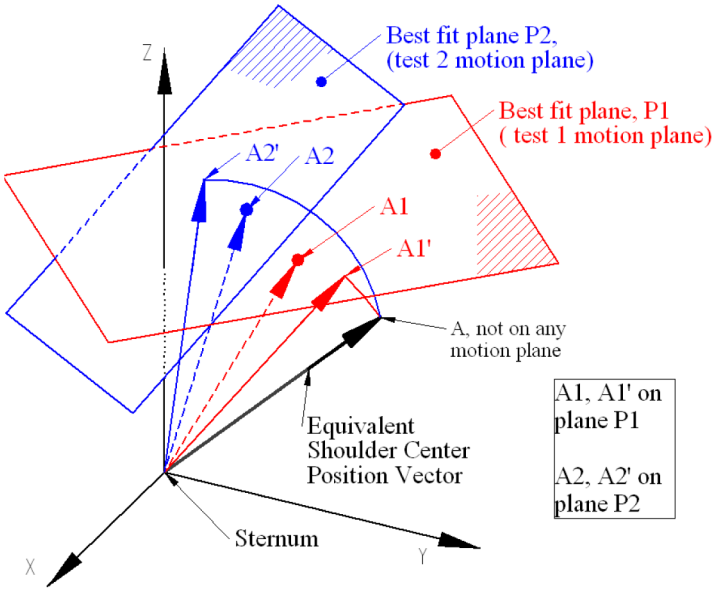

Fig. 2 Locating the shoulder center for each test. The equivalent shoulder center A is obtained by averaging the magnitudes and directions of the best-fit circle centers (A1 and A2). Point A does not lie in any motion plane. A1′ is the final shoulder center location for test 1 obtained by rotating the position vector of point A until it lies in the motion plane P1. A2′ lies in motion plane P2.

metic mean of the least-squares-fit radii gives the forearm length of the equivalent mechanism. The center of each best-fit circle gives the elbow position in a coordinate frame fixed at marker iii for the particular test and will henceforth be called the elbow. The motion of the elbow, rather than marker iii, with respect to the sternum frame is used to obtain the upper arm length and the shoulder joint position. A circle is fit in a least-squares sense to the elbow motion expressed in the sternum frame for each test. The arc length of the elbow motion varies significantly for pointing to different targets. The elbow-path length for reaching in the contralateral hemifield will be larger than that for reaching to a target in the ipsilateral hemifield. Circles fit to longer elbow paths will provide more accurate estimates of the upper arm length. Therefore, the upper arm length for the equivalent mechanism is a weighted average of the radii of the fit circles, with the weights based on the arc lengths of the corresponding elbow paths. Longer paths have higher weights. Note that the relative wrist paths are independent of the target location since each motion involves similar flexion/extension of the elbow joint. Thus, the arithmetic mean for the forearm length described above is justified.

The human shoulder does not remain stationary relative to the trunk during arm motion. Consequently, the elbow motion relative to the trunk will not be circular, and may be considered as a resultant of an upper-arm rotation about some center and a translation of that center relative to the trunk. Modeling the shoulder joint as a

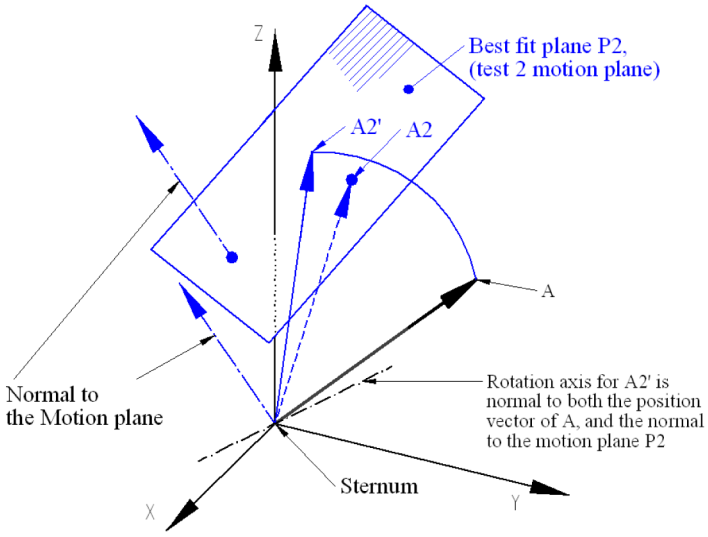

Fig. 3 Rotation axis for locating the unique shoulder center for each test. The axis passes through the sternum and is perpendicular to the position vector of the equivalent shoulder center and the normal to the corresponding motion plane.

single-DOF, fixed-axis revolute is a rough approximation necessitated by the nature of this analysis. The center of the best-fit circle to an elbow motion provides a poor estimate of the center location of such a 'shoulder-approximating' revolute joint. The following procedure, also illustrated in Figure 2, provides a better estimate. To locate a fixed shoulder center, it is required to fix the direction and magnitude of its position vector relative to the sternum-fixed frame. The circle fit to the elbow motion for each test gives a center in the motion plane for the test, e.g. points A1 and A2 in Figure 2. These are 3-dimensional position vectors expressed in the sternum-fixed frame XYZ in Figure 2. The 27 centers are combined into a single equivalent shoulder center by taking the weighted average of the directions and magnitudes of these vectors separately, and then combining the results. The same weights from the upper arm length computation are used. Point A in Figure 2 represents the equivalent shoulder center. Because of the averaging operation, the equivalent shoulder center does not lie in any of the 27 motion planes, in general. Therefore, for each test, the equivalent shoulder center vector is rotated until a unique shoulder center position in the test's motion plane is obtained, e.g. points A1′ and A2′ in Figure 2. This approach retains the length of the equivalent shoulder center position vector, and compromises only the small change in its direction. The rotation of the equivalent center's position vector is illustrated in Figure 3. The position vector of point A rotates about an axis passing through the sternum. To get the shoulder center for test 2, i.e. point A2, the axis of rotation is perpendicular to the position vector of A and the normal to the motion plane P2. In this way, the rotation axis for each test will pass through the sternum, but will have a different orientation. Next, the shoulder

Table 1 Inputs to the path-tracking algorithm.

Parameter	Value
Angle displacement	2°
Reduced angle displacement	1°
Permissible position error	0.5 cm
Permissible tangential error	25°
Limit for curvature and rate of change of curvature	1.5×10^{-3} cm^{-1}, cm^{-2}
Speed ratio limit	15

and elbow joint displacements, λ and μ respectively, for tracking the experimental paths are obtained via inverse kinematics. The forearm and upper arm lengths and the shoulder center determined above are used for this calculation. The experimental first-order speed ratios are obtained from the joint trajectories as

$$n = \frac{d\lambda}{d\mu} = \frac{\dot{\lambda}}{\dot{\mu}}, \tag{1}$$

where $\dot{\lambda}$ and $\dot{\mu}$ are the joint velocities of the shoulder and elbow obtained by numerically differentiating the joint displacements.

3.2 Model-Determined Speed Ratios

This section outlines the functioning of the path-tracking algorithm and the computation of the speed ratios. The fourth-order polynomial for the desired path, along with the arm-segment lengths and the shoulder center determined in the last section are inputs to the algorithm. Other inputs to the algorithm are the parameters listed in Table 1, which were constant for all tests and subjects.

To track the desired path, the tracking system starts from an initial pose corresponding to the initial position of the subject's arm, with the wrist on the desired path. The curvature properties, viz. the tangent direction and the curvature of the desired path are computed. Curvature theory [8] provides a way of mapping these values onto the shoulder-based first- and second-order speed ratios. The first-order speed ratio is defined by Equation 1, and the second-order speed ratio is $n' = \frac{dn}{d\mu}$. Next, the leading joint-angle displacement, λ, is chosen. If the curvature properties exceed the limits in Table 1, the reduced angle displacement is chosen. Otherwise, the standard angle displacement is employed. The subordinate (elbow) joint displacement μ is obtained via the second-order Taylor series

$$\mu = n\lambda + \frac{n'}{2}\lambda^2. \tag{2}$$

Second-order tracking is implemented because first-order tracking produces significant wrist oscillations about the desired path. If n' is greater than the ratio limit in Table 1, the elbow is chosen as the leading joint instead, and the inverse of Equation 2 is used. The speed ratio magnitude increases when the leading joint approaches a dwell, so the ratio limit detects this phenomenon. This joint switching strategy is critical for producing good tracking. The strategy agrees with recent studies supporting the leading joint hypothesis (LJH) [5]. The LJH states that in multi-articular limb motion there exists a leading joint, usually the proximal (shoulder) joint, that creates the foundation of the required motion by moving independent of the other joints. Based on this motion, the subordinate joint(s) move such that the required end-effector motion is obtained. The advantage of the LJH is that it allows the decomposition of the control problem into hierarchical components, which simplifies the control process [5]. For this reason, the algorithm chooses the shoulder joint as the leading joint, except when it is forced to switch according to the speed ratio limit.

As the mechanism advances through the computed joint displacements, the motion produces error in the tracking, such that the wrist no longer lies on the desired path. The angle displacement in Table 1 refers to the leading joint displacement after which the tracking system computes the tracking error by sensing the location of the *error point*, and the tangent direction of the desired path at the error point. The error point is the point on the desired path closest to the current wrist position. Two error parameters, viz. *position error* and *tangential error*, are computed. Position error is the distance between the error point and the current wrist position, while tangential error is the angle between the wrist path tangent and the desired path tangent at the error point. If the current position or tangential error exceeds the permissible limits specified in Table 1, path correction is accomplished by changing the wrist trajectory tangent direction such that further motion reduces the position error. New speed ratios corresponding to the corrected tangent are obtained. The process repeats until the desired path ends. The strategy of computing the speed ratios only when some error parameter is exceeded serves to reduce the computational load on the system. The modeling speed ratios are thus generated by the algorithm based on the geometric properties of the desired path.

4 Experiment and Modeling Comparison

The experimental paths for most tests were curves with low curvature. The algorithm, using second-order joint coordination, was able to track the paths to a high accuracy of 0.5 cm position error, for path lengths between 10 to 20 cm. Each motion was split into an outward motion toward the target and an inward motion back to the home position. Figures 4 and 5 show typical results. The experimental and modeling speed ratios for each were compared separately. Figure 4 shows the speed ratios plotted against the normalized arc length for all speeds for an inward motion from a light in the ipsilateral hemifield. Figure 5 shows the ratios for all

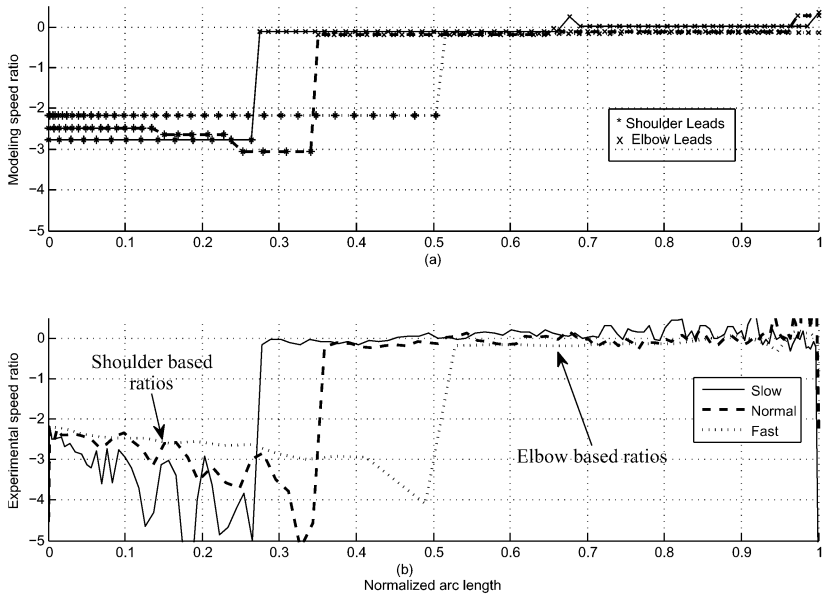

Fig. 4 Ipsilateral reaching: (a) the modeling first-order speed ratios for one subject pointing inward from light seven in Figure 1, with the right hand; (b) the experimental ratios for the same motion.

speeds for an outward motion to a light in the contralateral hemifield. Figures 4a and 5a show the modeling ratios determined by the algorithm for tracking the desired paths. In Figure 4a, a portion of the path is traversed with the shoulder leading, and the remainder with the elbow leading. The shoulder-based first-order speed ratio is defined by Equation (1), and the elbow-based ratio is its inverse. As indicated in Figure 4b, the shoulder- or elbow-based ratio is plotted for the corresponding portion of the experimental path. In Figure 5a, the entire path was traversed with the shoulder leading, hence Figure 5b plots all shoulder-based ratios.

The sharp jumps in the speed ratios in Figure 4 correspond to the elbow taking over as the leading joint for ipsilateral motions, a behavior observed for both hands in all subjects. This result agrees with the findings of Levin et al. [7] that the elbow exerts the maximum interaction torque on the shoulder for motions that involve small shoulder joint displacement and large elbow joint displacement, indicating an elbow-led movement. Dounskaia et al. [4] made the same observation in their experiment dealing with drawing movements. Dounskaia [5] proposed that the elbow becomes the leading joint for motions where the mechanical advantage of the shoulder cannot be used. The present work suggests a more fundamental explanation. A leading joint cannot achieve good tracking if it is approaching a dwell because any error in the leading joint motion will be amplified at the wrist. Further, if the leading joint is stationary, the motion of the subordinate joint cannot be derived from it. For ipsilateral reaching, the shoulder joint motion is small. Hence, the elbow takes over as the leading joint for ipsilateral reaching motions. A rapid in-

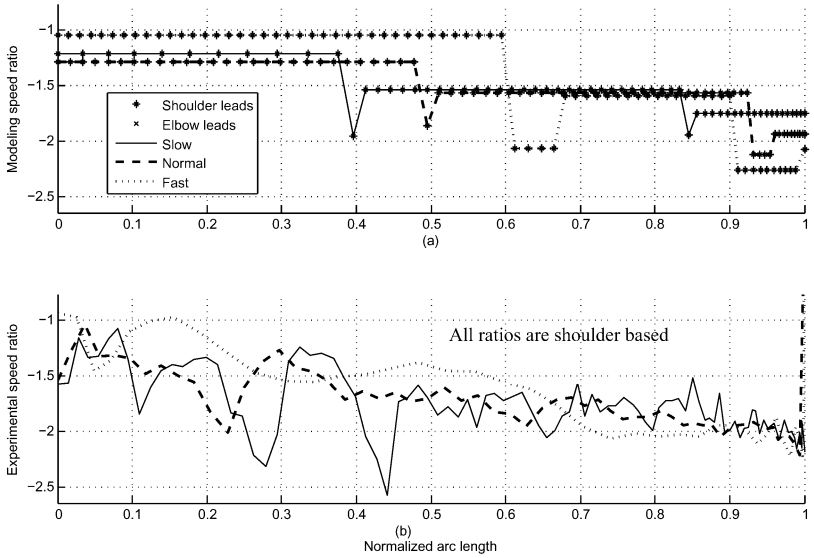

Fig. 5 Contralateral reaching: (a) the modeling first-order speed ratios for one subject pointing outward to light eight in Figure 1, with the left hand; (b) the experimental ratios for the same motion.

crease in the speed ratios indicates a joint's proximity to a dwell, and the algorithm successfully predicts this behavior via the speed ratio limit.

In contrast, the reaching movements in the contralateral hemifield do not exhibit change in the leading joint. Further, the experimental ratios in Figure 5b show gentle trends as compared to the sharp jumps in the ipsilateral hemifield. The modeling ratios follow similar trends, but in steps resulting from the algorithm's computationally frugal strategy of recalculating the ratios only when the error is exceeded. Each jump in the ratios indicates a correction and a subsequent recalculation of the speed ratios. The jumps in the speed ratios in Figure 5a are comparable to the amplitude of noise in the experimental data. Hence, the experimental data does not serve to validate or invalidate the idea of intermittent path correction. Additionally, no noticeable pattern emerged from analyzing the inward and outward motions separately.

5 Conclusions

This paper presents experimental validation of a planar, time-invariant inverse kinematic model for human motor control of reaching, and a path-tracking algorithm based on the time-invariant model. Experimental data was collected by measuring the arm motion of healthy individuals as they pointed to fixed targets in the horizontal plane at three self-selected speeds. An equivalent planar revolute-revolute

mechanism approximating the subject's arm was obtained through data analysis. The algorithm used the equivalent mechanism to successfully track the experimental paths closely. Second-order tracking is required to accurately match the experimental path, suggesting that motor planning may involve second-order joint coordination. The experimental first-order speed ratios for pointing to a target at three different speeds are similar, indicating time-invariant planning in the central nervous system. The algorithm correctly predicts the leading joint for motions in different hemifields. The experimental data and the model together corroborate the leading joint hypothesis by predicting elbow-led motions in the ipsilateral hemifield. Since the subordinate joint motion is derived from the motion of the leading joint, poor tracking results are obtained if a leading joint is near a dwell. This is because any error at the leading joint will be amplified at the wrist. Further, at a dwell, the subordinate joint motion cannot be derived from the stationary leading joint. These are more fundamental reasons for observed elbow-led motions in the ipsilateral hemifield than previously proposed.

Acknowledgement

This material is based upon work supported by the National Science Foundation under Grant No. IIS-0546456 to James Schmiedeler.

References

1. Ambike, S., Schmiedeler, J.P., Modeling time invariance in human arm coordination, in: J. Lenarčič, B. Roth (Eds.), *Advances in Robot Kinematics*, pp. 177–184. Springer, Dordrecht (2006).
2. Ambike, S., Schmiedeler, J.P., A methodology for implementing the curvature theory approach to path tracking with planar robots, *Mechanisms and Machine Theory*, in press (2007).
3. Crear, D.E., A study on time invariance in horizontal planar reaching movements, Masters Thesis, The Ohio State University (2007).
4. Dounskaia, N., Ketcham, C.J., Stelmach, G.E., Commonalities and differences in control of a large set of drawing movements, *Experimental Brain Research* **146**, 11–25 (2002).
5. Dounskaia, N., The internal model and the leading joint hypothesis: Implications for control of multi-joint movements, *Experimental Brain Research* **166**, 1–16 (2005).
6. Gander, W., Golub, G.H., Strebel, R., Fitting of circles and ellipses, *BIT Numerical Mathematics* **34**, 558–578 (1994).
7. Levin, O., Ouamer, M., Steyvers, M., Swinnen, S.P., Directional tuning effects during cyclic two-joint arm movements in the horizontal plane, *Experimental Brain Research* **141**, 471–484 (2001).
8. Lorenc, S.J., Stanisic, M.M., Hall Jr, A.S., Application of instantaneous invariants to the path tracking control problem of planar two degree-of-freedom systems: A singularity-free mapping of trajectory geometry, *Mechanism and Machine Theory* **30**, 883–896 (1995).